# Effects of Cholesterol and Adrenodoxin Binding on the Heme Moiety of Cytochrome P-450$_{scc}$: A Resonance Raman Study†

Motonari Tsubaki,* Atsuo Hiwatashi, and Yoshiyuki Ichikawa
*Department of Biochemistry, Kagawa Medical School, Miki-cho, Kita-gun, Kagawa 761-07, Japan*
*Received September 9, 1985; Revised Manuscript Received December 18, 1985*

ABSTRACT: The effects of cholesterol and adrenodoxin binding on resonance Raman spectra of cytochrome P-450$_{scc}$ in both oxidized and CO-reduced states were examined. Upon cholesterol binding, oxidized cytochrome P-450$_{scc}$ showed a significant shift of spin equilibrium from low-spin to high-spin state. Addition of adrenodoxin caused a complete conversion of cholesterol-bound oxidized cytochrome P-450$_{scc}$ to a pure high-spin state that was considered to be in the hexacoordinated state judged by the $\nu_{10}$ mode at 1620 cm$^{-1}$ and $\nu_3$ mode around 1485 cm$^{-1}$. Cholesterol in substrate binding site may oppose a linear and perpendicular binding of carbon monoxide to the reduced heme iron, leading to the distorted Fe–C–O linkage. This is based on the following observations: (1) an increase of the Fe–CO stretching frequency to 483 from 477 cm$^{-1}$ upon addition of cholesterol; (2) an enhanced photodissociability of bound carbon monoxide of CO complex of cytochrome P-450$_{scc}$ in the presence of cholesterol. As another aspect of the effect of cholesterol on the CO complex form of cytochrome P-450$_{scc}$, the enhanced stability of the native form ("P-450" form) was observed. There was no additional effect of reduced adrenodoxin on the Raman spectra of the CO-reduced form of cytochrome P-450$_{scc}$.

Side-chain cleavage of cholesterol to pregnenolone is the rate-limiting step in steroid hormone biosynthesis (Stone & Hechtor, 1954). This process is catalyzed by mitochondrial cytochrome P-450$_{scc}$,[1] together with its NADPH-specific electron transport system (adrenodoxin reductase plus adrenodoxin) (Lambeth et al., 1979, 1982). It is known that although the heme iron of cholesterol-free cytochrome P-450$_{scc}$ is fully low-spin state, cholesterol binding to the substrate binding site of cytochrome P-450$_{scc}$ causes the spin-state conversion from low to high (Lambeth et al., 1980, 1982).

Adrenodoxin, an iron–sulfur protein, forms 1:1 complexes with both NADPH-adrenodoxin reductase and cytochrome P-450$_{scc}$. While the binding of adrenodoxin and cholesterol to cytochrome P-450$_{scc}$ exhibits a strong positive cooperativity, adrenodoxin nevertheless binds to cholesterol-free cytochrome (Lambeth et al., 1980; Lambeth & Pember, 1983). During electron transfer, the complexes appear to function sequentially by "adrenodoxin shuttle mechanism" (Lambeth et al., 1979, 1982; Lambeth & Pember, 1983) rather than via a ternary complex of all three proteins (Kido & Kimura, 1979): i.e., adrenodoxin first forms its complex with and accepts an electron from adrenodoxin reductase, then dissociates, and finally forms a 1:1 complex with and transfers an electron to cytochrome P-450$_{scc}$. A total of six electrons and three oxygen molecules is necessary for the oxidative side-chain cleavage of cholesterol by this system.

Resonance Raman scattering from hemoproteins can provide some important informations on the structure of the heme moiety [Tsubaki & Yu, 1981; Tsubaki et al., 1981, 1982; see a review such as Spiro (1982)]. In recent Raman studies on the cytochrome P-450$_{scc}$–CO complex, we observed the resonance enhancement of Fe–CO stretching frequency and bound C–O stretching frequency at 477 and 1953 cm$^{-1}$, respectively (Tsubaki et al., 1984; Tsubaki & Ichikawa, 1985). This unusually low Fe–CO stretching frequency, compared to those of (carbonmonoxy)hemoglobin and myoglobin (507 and 512 cm$^{-1}$, respectively) (Tsubaki et al., 1982), was interpreted as a direct indication of a weaker Fe–CO bond strength caused by a cysteinyl thiolate ligand trans to CO and a linear and perpendicular coordination of CO to the heme (Tsubaki & Ichikawa, 1985).

In this study, we report the resonance Raman spectra of cytochrome P-450$_{scc}$ in oxidized and CO-reduced states and discuss the effects of cholesterol (substrate) and adrenodoxin binding on the heme moiety of both states.

## Materials and Methods

*Purification of Cytochrome P-450$_{scc}$.* Cytochrome P-450$_{scc}$ was purified as follows. Bovine adrenal glands were obtained from a local slaughterhouse. Their connective tissues and fat tissues were removed with scissors as much as possible, and then the glands were separated carefully into adrenocortexes and medullas. The capsules of the cortexes were scraped off with a razor. The mitochondrial fraction was obtained from the adrenocortexes by the method of Hiwatashi et al. (1976).

Adrenocortical mitochondria depleted of adrenodoxin and NADPH-adrenodoxin reductase with sonication were suspended in 10 mM potassium phosphate buffer (pH 7.4) containing 20% (v/v) glycerol and 1 mM EDTA. Sodium cholate was added to the suspension (about 12–16 mg of protein/mL) at the ratio of protein:sodium cholate of 2:1 (w/w). The solution was stirred for 45 min at 4 °C and, then, spun at 78740*g* (30 000 rpm) for 90 min on a Beckman L-8 ultra-

† This investigation was supported in part by Grants for Scientific Research from the Ministry of Education, Science, and Culture, Japan, and by grants-in-aid from The Shimabara Science Promotion Foundation and from The Naito Foundation.

* Author to whom correspondence should be addressed.

[1] Abbreviations: cytochrome P-450$_{scc}$, cytochrome P-450 in mitochondria of adrenal cortex which functions in cholesterol side-chain cleavage reaction; cytochrome P-450$_{cam}$, cytochrome P-450 obtained from *Pseudomonas putida* grown on D-camphor as the sole carbon source; cytochrome P-450$_{11\beta}$, cytochrome P-450 in mitochondria of adrenal cortex which functions in steroid 11$\beta$-hydroxylation; cytochrome P-450$_{LM2}$, the major phenobarbital-inducible cytochrome P-450 in rabbit liver microsomes; EDTA, ethylenediaminetetraacetic acid; SDS, sodium dodecyl sulfate.

0006-2960/86/0425-3563$01.50/0 

centrifuge. The supernatant was incubated at room temperature for 30 min and then mixed with a slurry of DEAE-cellulose previously equilibrated with 10 mM potassium phosphate buffer (pH 7.8) containing 20% (v/v) glycerol, 0.1% (v/v) Emulgen 913, 0.25% (w/v) sodium cholate, and 0.1 mM EDTA (buffer A). The slurry was poured into a glass column. After being packed, the column was washed extensively with buffer A (about 2000 mL) overnight. When a clear reddish band was formed in the bottom of the column, the column was treated with a 2000-mL linear gradient of NaCl concentration (0–0.3 M) in buffer A. The eluate was collected with 17-mL fractions automatically. Cytochrome P-450$_{scc}$ rich fractions were eluted during this treatment as a sharp peak and were combined and directly applied to a column of hydroxylapatite gel previously equilibrated with buffer A. The cytochrome was adsorbed at the top of the column as a clear red band. The column was washed succeedingly with 500 mL each of 10, 20, and 40 mM potassium phosphate buffer (pH 7.8) containing the same ingredients of buffer A. The cytochrome P-450$_{scc}$ was, then, eluted with 80 mM potassium phosphate buffer (pH 7.4) containing 20% glycerol, 0.1% Emulgen 913, 0.25% sodium cholate, and 0.1 mM EDTA. The eluate was dialyzed extensively against 10 mM potassium phosphate buffer (pH 6.5) containing 20% glycerol, 0.1% Emulgen 913, and 0.1 mM EDTA (buffer B) at 4 °C. The dialysate was applied to a column of CM-Sepharose CL-6B previously equilibrated with buffer B. The cytochrome was adsorbed in the column as a dark red band, and the column was washed with buffer B and then with 10 mM potassium phosphate buffer (pH 7.4) containing 20% glycerol, 0.1% Emulgen 913, and 0.1 mM EDTA. The cytochrome was desorbed by a 600-mL linear gradient of NaCl concentration (0–0.3 M) in 10 mM potassium phosphate buffer (pH 7.4) containing 20% glycerol, 0.1% Emulgen 913, and 0.1 mM EDTA. The eluate was collected with 10-mL fractions automatically, cytochrome P-450$_{scc}$ rich fractions were analyzed with SDS–polyacrylamide gel electrophoresis, and fractions with a single protein-staining band were combined.

SDS–polyacrylamide gel electrophoresis was performed as Laemmli (1970), and the molecular weight of cytochrome P-450$_{scc}$ was estimated to be 53 000.

*Depletion of Emulgen 913 from the Purified Cytochrome P-450$_{scc}$.* Emulgen 913 in purified sample was removed by adrenodoxin–Sepharose 4B column chromatography (Sugiyama et al., 1976; Chashchin et al., 1984). Cytochrome P-450$_{scc}$ was dialyzed extensively against 300 volumes of 10 mM potassium phosphate buffer (pH 7.4) containing 20% glycerol and 0.1 mM EDTA at 4 °C with several changes. The dialysate was loaded onto a column of adrenodoxin–Sepharose 4B previously equilibrated with the same buffer; the cytochrome was adsorbed at the top of the column as a reddish band. The column was washed with the equilibrating buffer (10 column volumes) followed by the same buffer containing 85 mM NaCl until the absorption at 280 nm of the eluate decreased lower than 0.025. The adsorbed cytochrome was eluted with the equilibrating buffer containing 0.20% sodium cholate and 300 mM NaCl. The eluate was collected, and peak fractions were combined and dialyzed against 10 mM potassium phosphate buffer containing 20% glycerol and 0.1 mM EDTA. The resulting sample was in a pure low-spin form and practically free from Emulgen 913 as judged by the absorption spectra in the ultraviolet region.

*Measurements of Optical Absorption Spectra of Cytochrome P-450$_{scc}$.* Optical absorption spectra of cytochrome P-450$_{scc}$ were measured on a Shimadzu UV-240 spectrophotometer equipped with an automatic wavelength calibrator (±0.3 nm). The temperature of the sample was maintained by a circulation of water from thermobath to water-jacketed cell holder.

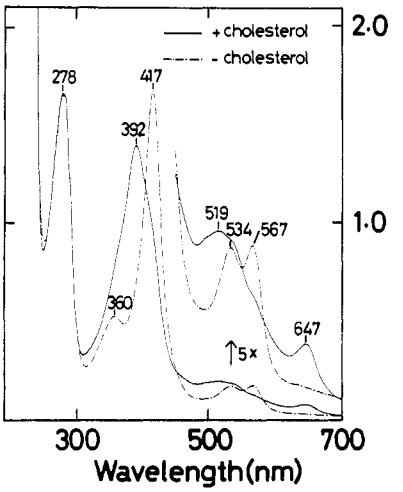


FIGURE 1: UV–visible absorption spectra of Emulgen 913 depleted cytochrome P-450$_{scc}$ after adrendoxin–Sepharose 4B column chromatography. One dotted line, cholesterol-free form; solid line, cholesterol-bound form (28.6 μM cholesterol). Cytochrome P-450$_{scc}$ concentration 12.6 μM in 10 mM potassium phosphate buffer containing 20% glycerol and 0.1 mM EDTA; temperature 10 °C.

*Measurements of Resonance Raman Spectra of Cytochrome P-450$_{scc}$.* Excitation wavelengths used for resonance Raman measurements were 441.6 nm from a He–Cd laser (Kimmon Electric, Model CD 4801R) and 457.9 and 488.0 nm from an Ar laser (NEC, Model GLG 3300); the spectra were recorded on a JASCO R-800D Raman spectrophotometer. Calibration of the Raman spectrophotometer was carried out with indene or fenchone as the standard. Sample solution in a cylindrical Raman cell was spun at 1000 rpm to minimize local heating, photodecomposition, and photodissociation. All spectral measurements were performed in 10 mM potassium phosphate buffer (pH 7.4) containing 20% (v/v) glycerol, 100 mM NaCl, and 0.1 mM EDTA at the protein concentration of 47.5 μM, otherwise indicated.

## RESULTS

*Oxidized Form.* Before the depletion of Emulgen 913, the cytochrome P-450$_{scc}$ sample was in pure low-spin form as judged by a visible absorption spectrum. In this stage, cytochrome P-450$_{scc}$ could not be converted to high-spin form even if a saturated amount of cholesterol was added. This is due to the inhibitory effect of Emulgen 913 against substrate binding (Kido et al., 1979). Thus, it was necessary to remove Emulgen 913 from the purified sample to study the effect of cholesterol binidng on the heme moiety. We employed an adrenodoxin–Sepharose 4B column to remove Emulgen 913; this technique has been successfully used for the final purification step of mitochondrial cytochromes P-450 such as cytochrome P-450$_{11\beta}$ and P-450$_{scc}$. The recovered enzyme from the adrenodoxin–Sepharose 4B column was in pure low-spin form, having absorption maxima at 567, 534, 417, 360 nm identical with those of cytochrome P-450$_{scc}$ in the presence of Emulgen 913 (0.1%) (Figure 1, one dotted chain line). The absence of Emulgen 913 in the sample was clearly indicated by the weak absorption intensity at 278 nm, which was lower than the Soret absorption at 417 nm, and the ratio of $A_{278}/A_{417}$ was comparable to, or even lower than, that of the cytochrome P-450$_{scc}$ sample purified in an other laboratory (Hasumi et al., 1984).

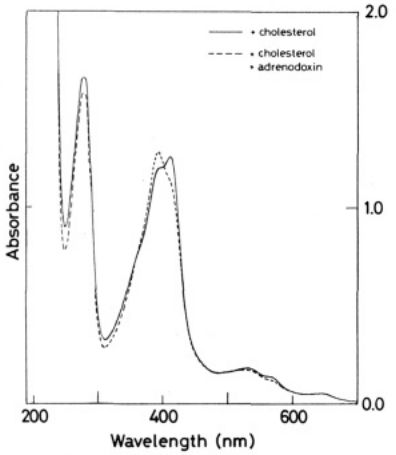


FIGURE 2: Effect of cholesterol and adrenodoxin on the ultraviolet–visible absorption spectra of oxidized cytochrome P-450$_{scc}$ (Emulgen 913 depleted form). Solid line, cytochrome P-450$_{scc}$ in the presence of cholesterol (28.6 $\mu$M); chain line, cytochrome P-450$_{scc}$ in the presence of both cholesterol and adrenodoxin (2.3 $\mu$M). Temperature 25 °C. Other conditions are the same as in Figure 1.

Upon addition of cholesterol[2] (28.6 $\mu$M; protein concentration 12.6 $\mu$M), the Emulgen-depleted cytochrome P-450$_{scc}$ could be converted to the high-spin form (approximately 50% high spin at 25 °C) (Figure 2, solid line). To make 100% high-spin form at this concentration, the temperature had to be lowered less than 10 °C (Figure 1, solid line). This strong temperature dependency of spin state was already reported (Katagiri et al., 1977).

The effect of adrenodoxin on the absorption spectra of cholesterol-bound cytochrome P-450$_{scc}$ can be clearly seen in Figure 2 (broken line). To maximize cholesterol-binding to cytochrome P-450$_{scc}$ at room temperature, we used relatively high ionic strength (100 mM NaCl) in the buffer throughout because the high ionic strength causes a decrease of apparent $K_d$ for cholesterol (Hanukoglu et al., 1981). But it is also known that the strength of the interaction between adrenodoxin and cytochrome P-450$_{scc}$ is reduced considerably at high ionic strength because their interaction is electrostatic (Hanukoglu et al., 1981). Nevertheless only a 2.26 $\mu$M concentration of adrenodoxin caused a significant increase of high-spin content as shown in Figure 2 (cytochrome P-450$_{scc}$ concentration 12.6 $\mu$M); this indicates that adrenodoxin has high affinity for cholesterol-bound cytochrome P-450$_{scc}$ even in this condition (100 mM NaCl) and forms a tight cholesterol–cytochrome P-450$_{scc}$–adrenodoxin complex to stabilize the cytochrome P-450$_{scc}$ heme almost completely in the high-spin state (Lambeth & Pember, 1983).

The resonance Raman spectra of cytochrome P-450$_{scc}$ for the higher frequency region (1300–1700 cm$^{-1}$) in various states as described earlier (but with a different protein concentraion, i.e., 47.5 $\mu$M) are presented in Figure 3. Excitation wavelength used was 441.6 nm from a He–Cd laser. As expected, in cholesterol-free state, the $\nu_{10}$ line[3] appeared at 1638 cm$^{-1}$ in the Raman spectrum, i.e., at the normal frequency of the ferric low-spin state. Other spin-state markers, $\nu_3$ and $\nu_{19}$ lines, can be seen at 1503 and 1584 cm$^{-1}$, respectively, characteristic for the ferric low-spin state (Figure 3, upper spectrum). When cholesterol was added (cholesterol concentration, 278.1 $\mu$M),

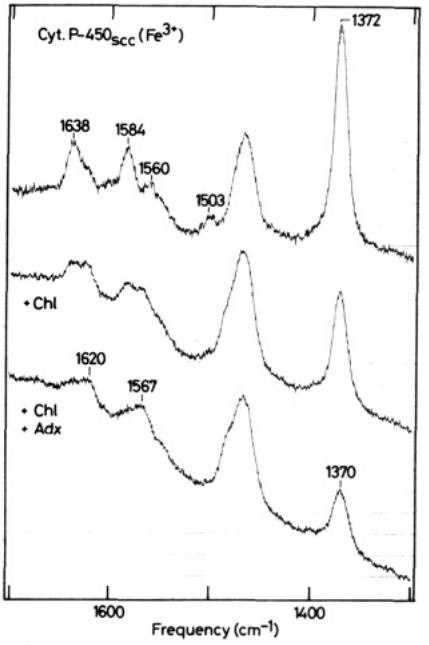


FIGURE 3: Effect of cholesterol and adrenodoxin on the higher frequency region resonance Raman spectra of oxidized cytochrome P-450$_{scc}$ in the absence of cholesterol (upper), in the presence of cholesterol (278.1 $\mu$M) (middle), and in the presence of both cholesterol (278.1 $\mu$M) and adrenodoxin (36.3 $\mu$M) (lower). Temperature of sample 10 °C. Cytochrome P-450$_{scc}$ concentration 47.5 $\mu$M; excitation wavelength 441.6 nm; laser power 18 mW at sample point; entrance slit width and height, 250 $\mu$m and 12 mm, respectively.

the cytochrome P-450$_{scc}$ heme spin state was converted almost in high spin (approximately 70% high spin at 10 °C) as judged by visible absorption spectra. In this condition the resonance Raman spectrum of the cytochrome exhibited the mixture of low- and high-spin states (Figure 3, middle spectrum). When 36.3 $\mu$M adrenodoxin was added additionally, the spectrum was almost devoid of low-spin signals (Figure 3, lower spectrum). The $\nu_{10}$ line shifted to 1620 cm$^{-1}$, and the $\nu_{19}$ line disappeared. The $\nu_3$ line shifted to around 1485 cm$^{-1}$ and was overlapped with a strong glycerol band at 1470 cm$^{-1}$. The $\nu_{11}$ line appeared at 1567 cm$^{-1}$. The frequencies of $\nu_3$, $\nu_{10}$, and $\nu_{11}$ are in accordance with the high-spin nature of the cytochrome P-450$_{scc}$ heme. When a 488.0-nm line from an Ar ion laser was employed for the excitation, essentially the same spectra were obtained for the cholesterol-free state and for both the cholesterol-bound and adrenodoxin-bound states, but with much reduced Raman intensities (data not shown). The decrease in frequency of the $\nu_4$ line by 2 cm$^{-1}$ in Figure 3 upon spin conversion from low to high state was not consistent with the result observed by Shimizu et al. (1981), in which they observed the frequency increase of $\nu_4$ line by 2 cm$^{-1}$ upon conversion from the low- to high-spin state. However, the decrease of the $\nu_4$ frequency upon spin conversion from low to high is the right direction judged by the empirical relationship observed for other hemoproteins.

We could observe only two Raman lines at 346 and 380 cm$^{-1}$ in the lower frequency region spectrum of the cholesterol-free form except for the lines from glycerol (Figure 4). Since oxidized adrenodoxin itself has Raman lines at 289, 346, and 391 cm$^{-1}$ with almost the same intensities as each other at this excitation wavelength (M. Tsubaki, unpublished observation; Adar et al., 1977), the major part of Raman intensities at 348 cm$^{-1}$ in the lower spectrum in Figure 4 is expected to be due to adrenodoxin assuming that the oxidized adrenodoxin in both the free and bound state has the same intensity ratios at 289, 346, and 391 cm$^{-1}$. Cytochrome P-450$_{scc}$–cholesterol–adre-

[2] The concentration of cholesterol is the maximum assuming cholesterol is fully solved. However, low solubility in aqueous solution and the nonspecific binding to protein other than the substrate binding site may reduce its actual concentration.

[3] The designation of porphyrin ring modes are based on Kitagawa et al. (1978) and Abe et al. (1978).

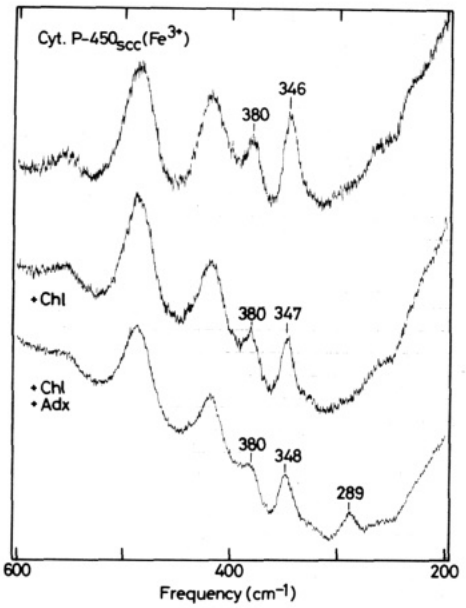


FIGURE 4: Effect of cholesterol and adrenodoxin on the lower frequency region resonance Raman spectra of oxidized cytochrome P-450$_{scc}$. Upper, in the absence of cholesterol; middle, in the presence of cholesterol; lower, in the presence of both cholesterol and adrenodoxin. Other conditions are the same as in Figure 3.

nodoxin complex stabilizes the cytochrome P-450$_{scc}$ heme completely in the high-spin state, and thus, the Raman intensities of the 346- and 380-cm$^{-1}$ modes of cytochrome P-450$_{scc}$ must be extremely weak in the Raman spectra of the high-spin state of cytochrome P-450$_{scc}$.

*Carbon Monoxide Reduced Form and Its Conversion to "P-420" Form in the Absence of Cholesterol.* The CO complex of reduced cytochrome P-450$_{scc}$ gave rise to the $\nu_4$ mode at 1368 cm$^{-1}$ (Figure 5, upper spectrum). This frequency is consistent with that reported by Shimizu et al. (1981) and close to those of the CO complexes of other cytochrome P-450 (Ozaki et al., 1978). This slightly lower frequency of the $\nu_4$ mode in the CO complex of reduced cytochrome P-450 compared to those of (carbonmonoxy)hemoglobin and -myoglobin (1372 and 1370 cm$^{-1}$, respectively) was considered due to the strong $\pi$ donor retained in its CO complex as the fifth ligand of heme iron (Ozaki et al., 1978).

During the laser illumination at room temperature (25 °C), this CO complex of reduced cytochrome P-450$_{scc}$ (cholesterol free) was converted to its denatured P-420 form even when the sample was kept in a spinning cell. Several hours of laser illumination caused an almost complete conversion of cytochrome P-450$_{scc}$ to the P-420 form as judged by visible absorption spectra. This conversion was clearly indicated in the Raman spectra by a significant broadening of the 1368-cm$^{-1}$ line toward lower frequency, suggesting the photodissociation of the CO complex of reduced P-420 (data not shown). It is well-known that the bound carbon monoxide molecule of "CO–P-420" is easily photodissociated (Shimada et al., 1979; Shimizu et al., 1981), and the resulting photodissociated (or reduced) P-420 is characterized by the appearance of the $\nu_4$ Raman line at 1357 cm$^{-1}$ with a very strong intensity (Figure 6, lower spectrum) (Ozaki et al., 1978; Champion et al., 1978).

In the lower frequency region spectra of the CO complex of reduced cytochrome P-450$_{scc}$, there is a strong Raman line at 477 cm$^{-1}$ which was assigned to the Fe–CO stretching frequency on the basis of the frequency shift by carbon monoxide isotope substitution (Figure 7, upper spectrum). This 477-cm$^{-1}$ line reduced its intensity upon conversion to the P-420 form. This intensity reduction was accompanied by the

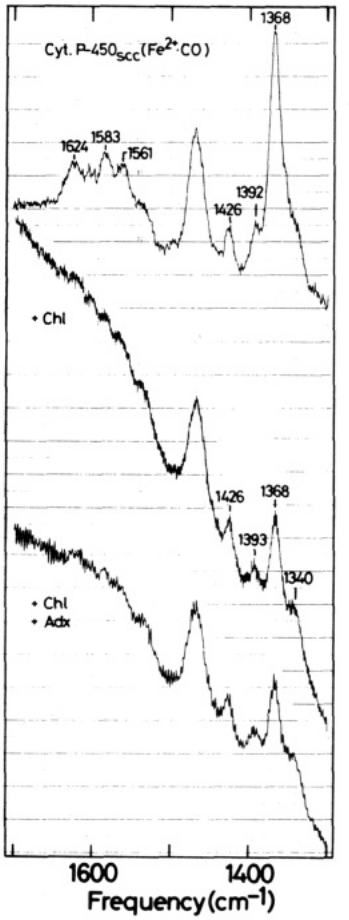


FIGURE 5: Effect of cholesterol and adrenodoxin on the higher frequency region spectra of cytochrome P-450$_{scc}$ (Fe$^{2+}$–CO). Upper, in the absence of cholesterol; middle, in the presence of cholesterol; lower, in the presence of both cholesterol and adrenodoxin. Other conditions are the same as in Figure 3.

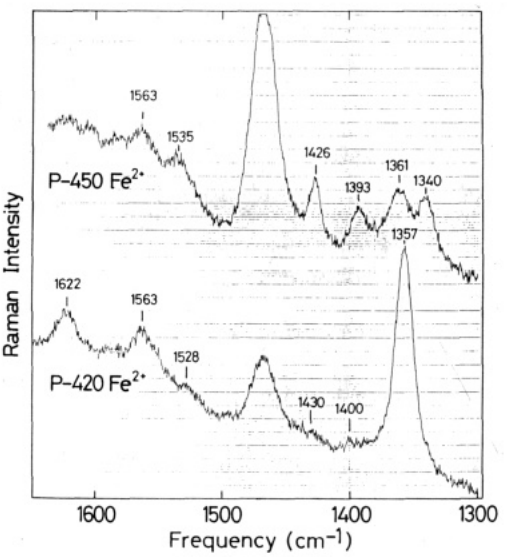


FIGURE 6: Resonance Raman spectra of cytochrome P-450$_{scc}$ in the native ("P-450") reduced state (upper spectrum) and in the denatured ("P-420") reduced state (lower spectrum). Both spectra were measured in the absence of cholesterol. Other conditions are the same as in Figure 3.

disappearance of the 318- and 280-cm$^{-1}$ lines. The Raman spectra of the P-420 form in the lower frequency region were characterized by the appearance of the 224-cm$^{-1}$ line. This line may be due to the photodissociated form of P-420 because there was a relatively sharp Raman line at 225 cm$^{-1}$ in the

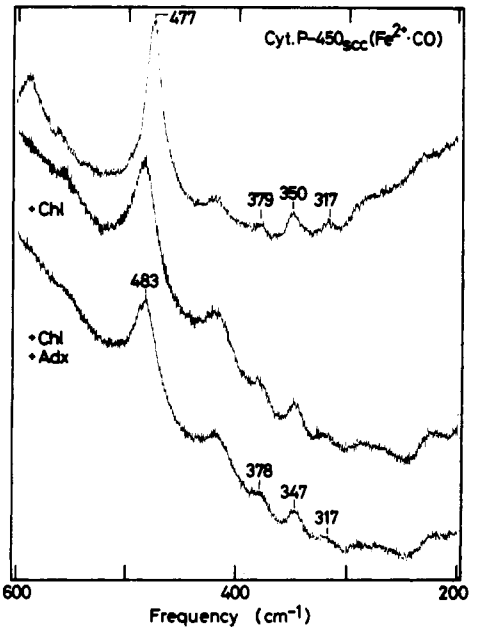


FIGURE 7: Effect of cholesterol and adrenodoxin on the lower frequency region Raman spectra of cytochrome P-450$_{scc}$ (Fe$^{2+}$–CO). Upper, in the absence of cholesterol; middle, in the presence of cholesterol; lower, in the presence of both cholesterol and adrenodoxin. Other conditions are the same as in Figure 3.

spectra of reduced P-420 (data not shown).

*Effect of Cholesterol and Adrenodoxin on the CO-Reduced Form.* Although the presence of cholesterol showed no effect on the visible absorption spectra of the CO-reduced form of cytochrome P-450$_{scc}$, there were some influences on the resonance Raman spectra. The most significant effect of cholesterol binding on the spectra of the CO-reduced form was an increase of the photodissociability of bound carbon monoxide. This phenomenon is clearly seen in Figure 5. The strong $\nu_4$ line at 1368 cm$^{-1}$ and several Raman lines around the 1550–1650-cm$^{-1}$ region reduced their intensities in the presence of cholesterol (278.1 $\mu$M), and the spectra in this higher frequency region became similar to that of reduced cytochrome P-450$_{scc}$ (compare Figure 5, middle spectrum, with Figure 6, upper spectrum). Since the spectrum of the reduced P-420 form or CO-photodissociated P-420 form was completely different from these spectra and since the visible absorption spectra after the measurements of Raman spectra of the cytochrome P-450$_{scc}$–CO complex showed no indication of the P-420 formation, this effect could not be ascribed to the denaturation to P-420. The effect of photodissociation in the Raman spectrum due to cholesterol binding was clearly observed in the lower frequency region also (Figure 7, middle spectrum). The Fe–CO stretching frequency at 477 cm$^{-1}$ lost its strong intensity slightly and showed a clear shift to 483 cm$^{-1}$ even considering the effect of the glycerol Raman lines at 484 and 420 cm$^{-1}$ with almost the same intensities as each other, the former overlapping with the Fe–CO stretching line. We could not detect any $\delta$ (Fe–C–O) bending vibration in the 500–600-cm$^{-1}$ region with and without cholesterol.

On the other hand, the addition of adrenodoxin to the cholesterol-bound CO-reduced form caused no additional effect on the resonance Raman spectra in both the higher and lower frequency region as shown in Figure 5 and 7, suggesting a weaker interaction between adrenodoxin and cholesterol-bound CO-reduced cytochrome P-450$_{scc}$. It must be noted that adrenodoxin was in the reduced form in this condition.

We tried to see the effect of cholesterol and adrenodoxin on the bound C–O stretching frequency. In the absence of cholesterol the bound C–O stretching frequency could be observed at 1953 cm$^{-1}$ by resonance Raman spectroscopy but with a much weak intensity compared to that of the Fe–CO stretching frequency (Tsubaki & Ichikawa, 1985). However, we could not detect any corresponding bound C–O stretching frequency around in this region in the presence of cholesterol alone or both cholesterol and adrenodoxin. This is presumably due to the strong photodissociability of carbon monoxide of the CO complex of cytochrome P-450$_{scc}$ in the presence of cholesterol.

## Discussion

The optical spectral change of the oxidized cytochrome P-450$_{scc}$ from low- to high-spin state upon addition of cholesterol is considered to indicate a direct binding of cholesterol to the substrate-binding site. This study presented clear evidence that cholesterol binding can affect a configuration around the oxidized heme of cytochrome P-450$_{scc}$ significantly. Adrenodoxin alone has no effect on the heme spin state, although there is a substantial interaction between adrenodoxin and substrate-free cytochrome P-450$_{scc}$ as evidenced by a successful preparation of cholesterol-free cytochrome P-450$_{scc}$ using adrenodoxin–Sepharose 4B column chromatography in the present study. Thus, adrenodoxin can affect the heme electronic structure only when cholesterol is bound to the substrate-binding site. In the context of Hasumi et al. (1984), binding of adrenodoxin to cholesterol-bound cytochrome P-450$_{scc}$ can induce a subtle movement of bound cholesterol in the vicinity of the heme leading to the complete spin conversion to high spin.

The $\nu_{10}$ mode of oxidized cytochrome P-450$_{scc}$ in the high-spin state observed at 1620 cm$^{-1}$, slightly higher than the value reported by Shimizu et al. (1981), is still in the reported range of the hexacoordinated high-spin complex (1608–1623 cm$^{-1}$) as suggested by Shimizu et al. (1981). The $\nu_3$ mode, which is overlapped with a glycerol Raman line at 1470 cm$^{-1}$, is expected to locate around 1485 cm$^{-1}$ as described under Results. This frequency is also in the range of the hexacoordinated complex (1475–1488 cm$^{-1}$). On the basis of the empirical relationship between the $\nu_{10}$ frequency and the coordinated atom (Teraoka & Kitagawa, 1980), Shimizu et al., 1981) suggested that the sixth ligand of the heme iron of cytochrome P-450$_{scc}$ in the high-spin state would be an oxygen atom, most likely the oxygen from a water molecule.

The resonance Raman spectrum in the lower frequency region (200–600 cm$^{-1}$) is quite informative since the Fe-ligand stretching modes of hemoproteins usually appear in this region. Indeed Champion et al. (1982) detected the Fe–S$^-$ stretching frequency at 351 cm$^{-1}$ by resonance Raman spectroscopy using isotopically labeled ($^{54}$Fe and $^{34}$S) samples of the oxidized cytochrome P-450$_{cam}$–substrate complex. Moreover, this $\nu$(Fe–S$^-$) stretching band disappeared upon depletion of the substrate, indicating that the substrate binding produces a significant change in the Fe–S$^-$ interaction. The 346-cm$^{-1}$ line in the Raman spectra of oxidized cytochrome P-450$_{scc}$ reduced its intensity upon depletion of cholesterol (substrate) contrary to the 351-cm$^{-1}$ mode in cytochrome P-450$_{cam}$, using glycerol Raman lines at 420 and 484 cm$^{-1}$ as internal standards. Since Champion et al. (1982) stated that resonance Raman spectra of the substrate-free cytochrome showed no evidence of the 351-cm$^{-1}$ mode for excitation throughout the Soret region and the 351-cm$^{-1}$ mode appeared only for excitation at 363.8 nm, the 346-cm$^{-1}$ mode in oxidized cytochrome P-450$_{scc}$ may be a porphyrin ring mode.

We had assigned Fe–CO stretching frequency of the CO complex of cytochrome P-450$_{scc}$ at 477 cm$^{-1}$ in the previous

paper on the basis of the frequency shift upon carbon monoxide isotope substitution, i.e., from 477 $cm^{-1}$ for $^{12}C^{16}O$ to 470 $cm^{-1}$ for $^{12}C^{18}O$ (Tsubaki & Ichikawa, 1985). This frequency is much lower than the corresponding frequencies in (carbonmonoxy)hemoglobin and -myoglobin at 507 and 512 $cm^{-1}$, respectively (Tsubaki et al., 1982). This unusually low frequency could be explained mainly in terms of the $d_\pi(Fe)$–$\pi^*(CO)$ interaction which is weaker in cytochrome P-$450_{scc}$ than in usual hemoproteins such as (carbonmonoxy)-hemoglobin and -myoglobin (Tsubaki & Ichikawa, 1985).

One may expect a stronger $d_\pi(Fe)$–$\pi^*(CO)$ interaction in the cytochrome P-450–CO complex than in other hemoproteins since the thiolate ($S^-$) ligand has a strong $\pi$ basicity that should cause a pronounced delocalization of $d_\pi(Fe)$ electrons to the $\pi^*(CO)$ orbital, in addition to a delocalization to the porphyrin $\pi^*$ ($e_g$) orbital. The stronger $d_\pi(Fe)$–$\pi^*(CO)$ interaction should cause a stronger Fe–CO bond strength, provided that $\sigma$-bonding between Fe and CO does not change. However, the previous (Tsubaki & Ichikawa, 1985) and present data indicate that the Fe–CO bond strength is actually weaker in cytochrome P-450 than in other hemoproteins. There are two explanations for this observation: (1) A weaker $\sigma$-bonding between Fe and CO in cytochrome P-450; (2) A weaker $d_\pi$-(Fe)–$\pi^*(CO)$ interaction in cytochrome P-450. The weaker $\sigma$-bonding between Fe and CO is unlikely since there is no compelling reason that the strong $\pi$-basicity of thiolate ion affects the $\sigma$-bonding between Fe and CO. In addition there is no indication of a stronger $\sigma$-donation from thiolate to iron, which may cause the weakening of the $\sigma$-bonding between Fe and CO. Calculations by Jung and Ristau (1977) showed a mixing of the Soret $\pi$–$\pi^*$ porphyrin transitions with charge-transfer transitions from an axial $\pi$-system [consisting of thiolate $\pi$-orbitals, CO $\pi$-orbitals, and the $d_\pi(Fe)$ orbitals] to the porphyrin $\pi^*$-orbitals. Their work suggested a direct role for the ligand trans to thiolate ligand in explaining the origin of hyper porphyrin (or "split Soret") spectrum. Therefore, it is very likely that carbon monoxide ligation trans to thiolate ligand may cause an unexpectedly large delocalization of $d_\pi(Fe)$ electrons to the porphyrin $\pi^*(e_g)$ orbitals, leading to the weaker $d_\pi(Fe)$–$\pi^*(CO)$ interaction.

Another factor that causes this unusually low Fe–CO stretching frequency is a linear and perpendicular bonding of carbon monoxide to the heme. It is known that the distorted Fe–C–O linkage with respect to the porphyrin ring causes the increase in the $\nu$(Fe–CO) stretching frequency with a concomitant decrease of bound C–O stretching frequency. X-ray diffraction studies revealed a distortion of Fe–C–O linkage in (carbonmonoxy)hemoglobin and -myoglobin; this distortion causes the increase in $\nu$(Fe–CO) frequency by 12–17 $cm^{-1}$ compared to that of the ferrous–carbonyl complex of heme 5 which is expected to have a linear and perpendicular Fe–C–O structure (Yu et al., 1983) and, therefore, to have a comparable Fe–C–O configuration with cytochrome P-$450_{scc}$ in the absence of cholesterol (Tsubaki & Ichikawa, 1985).

Recently Uno et al. (1985a) reported that the Fe–CO stretching frequency in the substrate-free cytochrome P-$450_{cam}$–CO complex lies at 464 $cm^{-1}$. Upon addition of substrate, camphor, the Fe–CO stretching frequency shifted to 481 $cm^{-1}$ and to 483 $cm^{-1}$ upon forming a bimolecular complex with putidaredoxin, and this frequency shift toward higher frequency was accompanied by a concomitant decrease of bound C–O stretching frequency from 1963 $cm^{-1}$ to 1940 and 1932 $cm^{-1}$, respectively.

As seen in Figure 8, our previous data and those of Uno et al. (1985) can be plotted along a line parallel to the one ob-

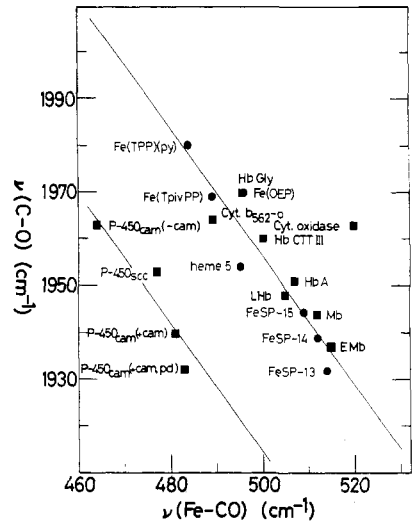


FIGURE 8: Fe–CO stretching frequency vs. C–O stretching frequency plots for various ferrous–heme–carbonyl complexes. (■) Data points for native heme proteins: glycera hemoglobin (Hb Gly), cytochrome $b_{562}$–$o$ complex (Cyt. $b_{562}$–$o$), cytochrome oxidase (Cyt. oxidase), elephant myoglobin (EMb), cytochrome P-$450_{cam}$ (P-$450_{cam}$). Data taken from Carson et al. (1985), Uno et al. (1985b), Argade et al. (1984), Kerr et al. (1985), Uno et al. (1985a), respectively. (●) Data points for various heme model complexes. Other data points were cited previously in Tsubaki and Ichikawa (1985).

tained for various ferrous heme–carbonyl complexes with a nitrogen atom as a fifth ligand. The departure of these two lines is probably not due to the Fe–C–O configuration but due to the differences in bonding nature between heme iron and fifth ligands (Tsubaki & Ichikawa, 1985).

From this parallelism we can speculate that substrate (camphor or cholesterol) binding causes a distortion of Fe–C–O linkage with respect to porphyrin ring on the basis of our previous proposal, i.e., as the distal steric hindrance increases, the $\nu$(Fe-CO) frequency increases with a concomitant decreasing of the bound $\nu$(C–O) frequency (Tsubaki & Ichikawa, 1985). It is very likely that almost the same mechanism is operative on Fe–C–O linkage in the CO complex of cytochrome P-$450_{cam}$ as in the cytochrome P-$450_{scc}$ complex upon substrate binding. Indeed the increase of Fe–CO stretching frequency by 6 $cm^{-1}$ in the presence of cholesterol, as observed in the present study, is a right direction in view of our previous proposal. It is known that the cholesterol-binding site is so close to the heme that C-22 of the cholesterol side chain is at the very vicinity of heme iron when cholesterol is bound, from a series of studies using synthesized steroid derivatives having the potential to interact with both the substrate binding site and the heme iron catalytic site of the enzyme (Sheets & Vickery, 1982, 1983a,b). Thus, it is very likely that the side-chain group of cholesterol opposes a linear and perpendicular binding of carbon monoxide to the heme iron of cytochrome P-$450_{scc}$.

An increased photodissociability of carbon monoxide from the CO complex of cytochrome P-$450_{scc}$ upon addition of cholesterol can be easily understood in this context. It is known that the electronic excitation at the porphyrin ring by the illumination of laser light at the Soret or Q ($\alpha$ and $\beta$) bands can affect the $d_\pi(Fe)$–$\pi^*(CO)$ interaction indirectly through the $d_\pi(Fe)$–$\pi^*$ (porphyrin) orbital interaction, leading to the photodissociation of the sixth ligand, carbon monoxide (Kitagawa et al., 1976; Tsubaki et al., 1982). In the distorted Fe–C–O configuration, the contribution of $\sigma$-type [$d_{z^2}(Fe)$–$\pi^*(CO)$] interaction may decrease significantly in the Fe–CO bond due to the bonding geometry, and the resulting increase

of $\pi$-type [$d_\pi$(Fe)–$\pi^*$(CO)] interaction in the Fe–CO bond may be the reason of the enhanced photodissociability upon cholesterol binding.

Another aspect of the effect of cholesterol on the CO complex of cytochrome P-450$_{scc}$ was the enhanced stability of the native ("P-450") state. Without cholesterol the CO complex of cytochrome P-450$_{scc}$ became its denatured form (CO complex of P-420) steadily as described. To the contrary, in the presence of cholesterol, the CO complex of cytochrome P-450$_{scc}$ was extremely stable for more than several hours when kept irradiated by laser light at room temperature (data not shown). To reveal the nature of this effect is beyond our scope in the present study. We can only say at this stage that cholesterol bound to the substrate-binding site may stabilize the tertiary structure around the heme.

The absence of the additional effect of adrenodoxin in the resonance Raman spectra of the CO-reduced form of cytochrome P-450$_{scc}$ is noteworthy. It must be noted that adrenodoxin is in the reduced form in this experimental condition. However, it is known that the redox state of adrenodoxin does not appear to have major effects on its association with cytochrome P-450$_{scc}$; reduction of adrenodoxin actually results in a slight weakening, by a factor of 2, of the interaction with both oxidized and reduced cytochrome P-450$_{scc}$ (Lambeth & Pember, 1983).

There is no available data to estimate the interaction between adrenodoxin and cholesterol-bound CO-reduced cytochrome P-450$_{scc}$ other than the present study. However, from the viewpoint of a physiological mechanism of steroidogenic electron transport, a stronger interaction between adrenodoxin and the cholesterol-bound CO-reduced form must be favored, because the cholesterol-bound CO-reduced form can be considered as a nice model for an oxygenated intermediate complex during the initial phase of the side-chain cleavage reaction.

**Registry No.** Cytochrome P-450, 9035-51-2; cholesterol, 57-88-5.

## REFERENCES


Abe, M., Kitagawa, T., & Kyogoku, Y. (1978) *J. Chem. Phys. 69*, 4526–4534.

Adar, F., Blum, H., Leigh, J. S., Jr., Ohnishi, T., Salerno, J. C., & Kimura, T. (1977) *FEBS Lett. 84*, 214–216.

Argade, P. V., Ching, Y. C., & Rousseau, D. L. (1984) *Science (Washington, D.C.) 225*, 329–331.

Carson, S. D., Constantinidis, I., Satterlee, J. D., & Ondrias, M. R. (1985) *J. Biol. Chem. 260*, 8741–8745.

Champion, P. M., Gunsalus, I. C., & Wagner, G. C. (1978) *J. Am. Chem. Soc. 100*, 3743–3751.

Champion, P. M., Stallard, B. R., Wagner, G. C., & Gunsalus, I. C. (1982) *J. Am. Chem. Soc. 104*, 5469–5472.

Chashchin, V. L., Vasilevsky, V. I., Shkumatov, V. M., & Akhrem, A. A. (1984) *Biochim. Biophys. Acta 787*, 27–38.

Hanukoglu, I., Spitesberg, V., Bumpus, J. A., Dus, K. M., & Jefcoate, C. R. (1981) *J. Biol. Chem. 256*, 4321–4328.

Hasumi, H., Yamakura, F., Nakamura, S., Suzuki, K., & Kimura, T. (1984) *Biochim. Biophys. Acta 787*, 152–157.

Hiwatashi, A., Ichikawa, Y., Maruya, N., Yamano, T., & Aki, K. (1976) *Biochemistry 15*, 3082–3090.

Jung, C., & Ristau, O. (1977) *Chem. Phys. Lett. 49*, 103–108.

Katagiri, M., Takikawa, O., Sato, H., & Suhara, K. (1977) *Biochem. Biophys. Res. Commun. 77*, 804–809.

Kerr, E. A., Yu, N.-T., Bartnicki, D. E., & Mizukami, H. (1985) *J. Biol. Chem. 260*, 8360–8365.

Kido, T., & Kimura, T. (1979) *J. Biol. Chem. 254*, 11806–11815.

Kido, T., Arakawa, M., & Kimura, T. (1979) *J. Biol. Chem. 254*, 8377–8385.

Kitagawa, T., Kyogoku, Y., Iizuka, T., & Saito, M. I. (1976) *J. Am. Chem. Soc. 98*, 5169–5173.

Kitagawa, T., Abe, M., & Ogoshi, H. (1978) *J. Chem. Phys. 69*, 4516–4525.

Laemmli, U. K. (1970) *Nature (London) 227*, 680–685.

Lambeth, J. D., & Pember, S. O. (1983) *J. Biol. Chem. 258*, 5596–5602.

Lambeth, J. D., Seybert, D. W., & Kamin, H. (1979) *J. Biol. Chem. 254*, 7255–7264.

Lambeth, J. D., Seybert, D. W., & Kamin, H. (1980) *J. Biol. Chem. 255*, 138–143.

Lambeth, J. D., Seybert, D. W., Lancaster, J. R., Jr., Salerno, J. C., & Kamin, H. (1982) *Mol. Cell. Biochem. 45*, 13–31.

Ozaki, Y., Kitagawa, T., Kyogoku, Y., Imai, Y., Hashimoto-Yutsudo, C., & Sato, R. (1978) *Biochemistry 17*, 5826–5831.

Sheets, J. J., & Vickery, L. E. (1982) *Proc. Natl. Acad. Sci. U.S.A. 79*, 5773–5777.

Sheets, J. J., & Vickery, L. E. (1983a) *J. Biol. Chem. 258*, 1720–1725.

Sheets, J. J., & Vickery, L. E. (1983b) *J. Biol. Chem. 258*, 11446–11452.

Shimada, H., Iizuka, T., Ueno, R., & Ishimura, Y. (1979) *FEBS Lett. 98*, 290–294.

Shimizu, T., Kitagawa, T., Mitani, F., Iizuka, T., & Ishimura, Y. (1981) *Biochim. Biophys. Acta 670*, 236–242.

Spiro, T. G. (1982) in *Iron Porphyrins, Part II* (Lever, A. B. P., & Gray, H. B., Eds.) pp 89–159, Addison-Wesley, Reading, MA.

Stone, D., & Hechtor, O. (1954) *Arch. Biochem. Biophys. 51*, 457–469.

Sugiyama, T., Miura, R., & Yamano, T. (1976) in *Iron and Copper Proteins* (Yasunobu, K., Mower, H. F., & Hayaishi, O., Eds.) pp 290–302, Academic, New York.

Teraoka, J., & Kitagawa, T. (1980) *J. Phys. Chem. 84*, 1928–1935.

Tsubaki, M., & Yu, N.-T. (1981) *Proc. Natl. Acad. Sci. U.S.A. 78*, 3581–3585.

Tsubaki, M., & Yu, N.-T. (1982) *Biochemistry 21*, 1140–1144.

Tsubaki, M., & Ichikawa, Y. (1985) *Biochim. Biophys. Acta 827*, 268–274.

Tsubaki, M., Srivastava, R. B., & Yu, N.-T. (1981) *Biochemistry 20*, 946–952.

Tsubaki, M., Srivastava, R. B., & Yu, N.-T. (1982) *Biochemistry 21*, 1132–1140.

Tsubaki, M., Matsusaka, K., & Ichikawa, Y. (1984) *Raman Spectrosc. Proc. Int. Conf., 9th*, 752–753.

Uno, T., Nishimura, Y., Makino, R., Iizuka, T., Ishimura, Y., & Tsuboi, M. (1985a) *J. Biol. Chem. 260*, 2023–2026.

Uno, T., Nishimura, Y., Tsuboi, M., Kita, K., & Anraku, Y. (1985b) *J. Biol. Chem. 260*, 6755–6760.

Yu, N.-T., Kerr, E. A., Ward, B., & Chang, C. K. (1983) *Biochemistry 22*, 4534–4540.